

# Network analysis of online bidding activity

I. Yang<sup>1</sup>, E. Oh<sup>1</sup> and B. Kahng<sup>1,2</sup>

<sup>1</sup>*School of Physics and Center for Theoretical Physics,  
Seoul National University, Seoul 151-747, Korea*

<sup>2</sup>*Center for Nonlinear Studies, Los Alamos National Laboratory, Los Alamos, New Mexico 87545.*

(Dated: November 20, 2018)

With the advent of digital media, people are increasingly resorting to online channels for commercial transactions. Online auction is a prototypical example. In such online transactions, the pattern of bidding activity is more complex than traditional offline transactions; this is because the number of bidders participating in a given transaction is not bounded and the bidders can also easily respond to the bidding instantaneously. By using the recently developed network theory, we study the interaction patterns between bidders (items) who (that) are connected when they bid for the same item (if the item is bid by the same bidder). The resulting network is analyzed by using the hierarchical clustering algorithm, which is used for clustering analysis for expression data from DNA microarrays. A dendrogram is constructed for the item subcategories; this dendrogram is compared with a traditional classification scheme. The implication of the difference between the two is discussed.

PACS numbers: 89.75.Hc, 89.65.Gh, 89.75.-k

## I. INTRODUCTION

Electronic commerce (e-commerce) refers to any type of business of commercial transaction that involves information transfer across the Internet. Online auction, a synergetic combination of the Internet supported by instantaneous interactions and traditional auction mechanisms, has rapidly expanded over the last decade. Owing to this rapid expansion and the importance of online auctions, very recently researchers have begun to pay attention to the various aspects of online auctions [1, 2, 3, 4, 5, 6, 7]. According to recent studies based on empirical data obtained from eBay.com, it was discovered that the online auction system is driven by a self-organized process, involving almost all the agents that participate in a given auction activity. For example, the total number of bids placed for a single item or category and the bid frequency submitted by each agent follow power-law distributions [5]. Further, the bidding process occurring in online auctions has been successfully described through the stochastic rate equation [6]. Thus, understanding of the bidding activities in online auctions is a highly attractive topic for the statistical physics community.

The remarkable connection between *beer and diapers* discovered in 1992 by Blischok et al. [8] has significantly improved profits. They analyzed the correlation between items sold at a drug store during a particular time interval between 5 p.m. and 7 p.m.. They found a strong correlation between the two items, which had never been noticed by the retailer earlier. This correlation arises from the fact that fathers in families tend to buy beer when they are told by their wives to buy diapers while returning home. This discovery, which is considered as a pioneering work of data mining, compelled drug stores to redesign their displays; this resulted in an increase in beer sales.

In online auctions, most of the limitations hampering traditional offline auctions, such as spatial and temporal constraint have virtually disappeared. Thus, it would be interesting to investigate how the bidding pattern of online auctions has changed from the traditional one. On the other hand, recently, considerable attention have been focused on complex network problems as an interdisciplinary subject [9, 10, 11]. Diverse computational methods to find clusters within large-scale networks have been introduced (for example, see Refs. [12, 13, 14, 15, 16]). Thus, by combining these two issues, in this study, we investigate the pattern emerging from the interactions between individual bidders or items in online auctions by using the recently developed network theory. The resulting network provides information on the bidding pattern of individual bidders as well as the correlation between different item subcategories. Moreover, we construct a dendrogram for these subcategories and compare it with a traditional classification scheme based on off-line transactions. For the purpose, we use an algorithm applied for clustering analysis for the expression data from a DNA microarray experiment in biological systems [17]. The dendrogram thus obtained is consumer-oriented, reflecting the pattern of an individual bidder's activities. Thus, it can be used for increasing profits by providing consumers with a link between the items, which should interest the consumers.

Our study is based on empirical data [5] collected from <http://www.eBay.com>. The dataset comprises all the auctions that ended in a single day, July 5, 2001, and includes 264,073 auctioned items grouped into 18 categories and 192 subcategories. The number of distinct agents that participated in these merchandize was 384,058.

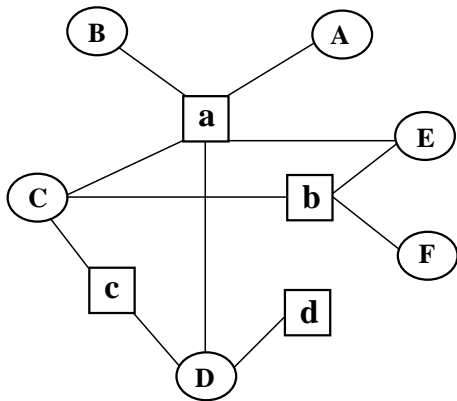


FIG. 1: A schematic illustration of a bipartite network of an online auction. Bidders and items are represented by ellipses with  $\{A, B, \dots, F\}$  and squares with  $\{a, b, c, d\}$ , respectively. Bidders A and B are connected via item a which they bid for. Items a and b are connected via bidders C and E who bid for both items a and b.

	$N$	$L$	$C_{\text{iso}}$
Bidder network	338,478	1,208,236	22,883
Item network	122,827	813,687	3,851

TABLE I: The numbers of vertices  $N$ , edges  $L$ , and isolated clusters  $C_{\text{iso}}$  for the bidder and the item networks.

## II. TOPOLOGIES OF BIDDER AND ITEM NETWORKS

The data contain the information on which bidder bids for which item via their unique user ID. Thus, we can construct a bipartite network comprising two disjoint sets of vertices, bidders and items, as shown in Fig. 1. The bipartite network can be converted to a single species of network such as the bidder or the item network, as shown in Figs. 2(a) and 2(b), respectively. The bidder and item networks can have edges with weight. For example, bidders C and D in Fig. 1 are connected twice through items a and c. Hence, the edge between C and D has weight 2. Similarly, items a and b are connected twice through bidders C and E. Thus, the edge between vertices a and b in the item network has weight 2. Statistics describing the topology of the entire network and the giant component of the bidder and the item network are listed in Table I and Table II, respectively.

Next, we characterize the structure of the bidder and item networks. First, we regard each network as a binary network, neglecting the weight of each edge. The network configuration can be described by the adjacent matrix  $\{a_{ij}\}$ ; its component is 1 when two vertices  $i$  and  $j$  are connected and 0 otherwise. Then, degree  $k_i$  of vertex  $i$  is  $k_i = \sum_j a_{ij}$ , which is the number of edges connected to it. We find that the degree distribution exhibits a power-law behavior asymptotically for both the bidder and item networks,  $P_d(k) \sim k^{-\gamma}$ . The degree exponent

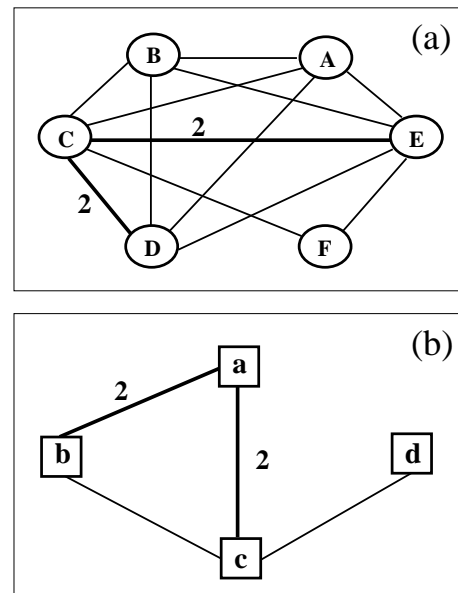


FIG. 2: Bidder network (a) and item network (b) converted from the bipartite network shown in Fig. 1. Thick edges have weight 2, while the other edges have unit weight for both (a) and (b).

	$N$	$L$	$\langle k \rangle$	$\langle d \rangle$
Bidder network	267,414 (79%)	2,245,794 (93%)	8.4	8.15
Item network	112,240 (91%)	695,281 (85%)	12.4	7.69

TABLE II: Statistics of the giant component of the bidder and item networks. The number of vertices is denoted by  $N$ ; edges,  $L$ ; mean degree,  $\langle k \rangle$ ; and mean distance between two vertices,  $\langle d \rangle$ .

$\gamma$  is estimated to be  $\gamma_B \approx 3.0$  for the bidder network and  $\gamma_I \approx 2.0$  for the item network, as shown in Fig. 3.

Second, strength  $s_i$  of vertex  $i$  is the sum of the weights of each edge connected to it. That is,  $s_i = \sum_j a_{ij} w_{ij}$ , where  $w_{ij}$  is the weight of the edge between vertices  $i$  and  $j$ . The strength distributions of the bidder and item networks also exhibit power-law behaviors asymptotically as  $P_s(s) \sim (s + s_0)^{-\eta}$  where  $\eta_B \approx 4.0$  for the bidder network and  $\eta_I \approx 3.5$  for the item network, as shown in Fig. 4.  $s_0$  is constant. Strength and degree of a given vertex exhibit an almost linear relationship  $s(k) \sim k^\zeta$  with  $\zeta \approx 0.95$ ; however, large fluctuations are observed for large  $k$  in Fig. 5.

Third, we measure the mean nearest-neighbor degree function  $\langle k_{\text{nn}} \rangle(k)$ . The mean degree of the nearest-neighbor vertices of a given vertex  $i$  with degree  $k$  is measured as follows:

$$k_{i,\text{nn}} = \left( \sum_j a_{ij} k_j \right) / k_i. \quad (1)$$

The average of  $k_{i,\text{nn}}$  over the centered vertex with degree

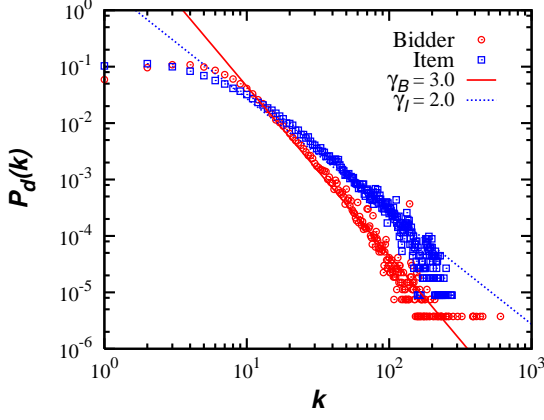


FIG. 3: Degree distribution  $P_d(k)$  as a function of degree  $k$ . Both display power-law behaviors  $P_d(k) \sim k^{-\gamma}$  with  $\gamma_B \approx 3.0$  for the bidder network and  $\gamma_I \approx 2.0$  for the item network. Solid lines are guidelines with slopes of 3.0 and 2.0 for the bidder and item networks, respectively.

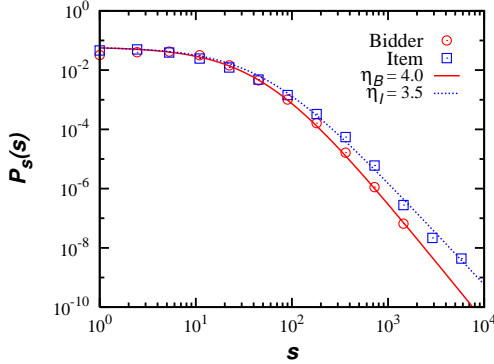


FIG. 4: Strength distributions  $P_s(s)$  as a function of strength  $s$  for the bidder and item networks. Asymptotically, they display a generalized power-law behavior  $P_s(s) \sim (s + s_0)^{-\eta}$ . The exponent is estimated to be  $\eta_B \approx 4.0$  for the bidder network and  $\eta_I \approx 3.5$  for the item network.  $s_0 = 51$  is used for the bidder network and  $s_0 = 52$  for the item network.

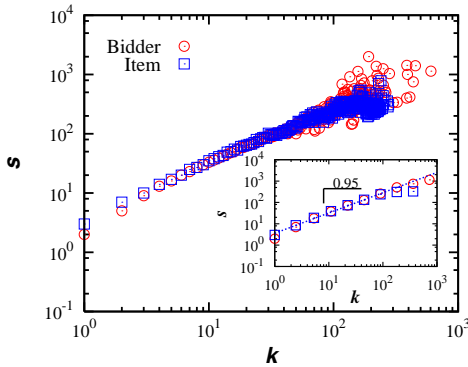


FIG. 5: The relation between strength  $s$  and degree  $k$  of each vertex. They show an almost linear relationship,  $s \sim k^\zeta$  with  $\zeta \approx 0.95$  for both the bidder ( $\circ$ ) and the item ( $\square$ ) network. Inset: Replot of  $s$  vs.  $k$  using the log-bin data.

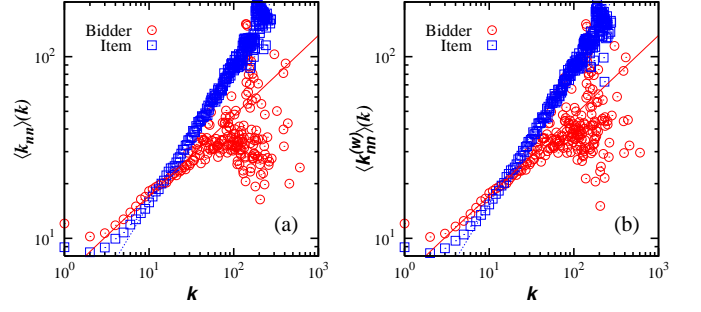


FIG. 6: The mean nearest-neighbor degree function  $\langle k_{nn} \rangle(k)$  ( $\circ$ ) and its weighted version  $\langle k_{nn}^{(w)} \rangle(k)$  ( $\square$ ) as a function of the degree  $k$  of a centered vertex for the bidder network (a) and the item network (b). Solid line, obtained from a least-square-fit, has a slope of 0.44 for the bidder network (a) and 0.77 for the item network (b). Both the networks are assortatively mixed.

$k$  is taken to obtain  $\langle k_{nn} \rangle(k)$ . For the weighted network, formula (1) is replaced following the formula [18]:

$$k_{i,nn}^{(w)} = \frac{1}{s_i} \sum_j a_{ij} w_{ij} k_j. \quad (2)$$

From this equation,  $\langle k_{nn}^{(w)} \rangle(k)$  can be similarly obtained. It is found that the functions  $\langle k_{nn} \rangle(k)$  and  $\langle k_{nn}^{(w)} \rangle(k)$  increase with the degree  $k$  of the centered vertex for both the bidder and item networks irrespective of the binary or weighted versions. That is, both the networks are assortatively mixed, implying that *active bidders tend to simultaneously bid for common items, thereby attractive items are also connected via such active bidders*.

Fourth, the local clustering coefficient  $c_i$  is the density of transitive relationships, and is defined as the number of triangles formed by its neighbors, which are cornered at vertex  $i$ , divided by the maximum possible number of neighbors,  $k_i(k_i - 1)/2$ . That is,

$$c_i = \frac{2}{k_i(k_i - 1)} \sum_{j,h} a_{ij} a_{ih} a_{jh}. \quad (3)$$

The average of  $c_i$  over the vertices with degree  $k$  is called the clustering coefficient function  $c(k)$ . For weighted networks, a similar clustering coefficient  $c_i^{(w)}$  is defined [18] as

$$c_i^{(w)} = \frac{1}{s_i(k_i - 1)} \sum_{j,h} \frac{w_{ij} + w_{ih}}{2} a_{ij} a_{ih} a_{jh}. \quad (4)$$

The average of  $c_i^{(w)}$  over the cornered vertices with degree  $k$  is similarly defined and denoted as  $c^{(w)}(k)$ . For the bidder network, the clustering coefficient functions  $c(k)$  and  $c^{(w)}(k)$  decrease with respect to  $k$  as shown in Fig.7(a); they exhibit large fluctuations for large  $k$ , implying that the bidder network is hierarchically organized. For the item network, however, both  $c(k)$  and  $c^{(w)}(k)$  are almost

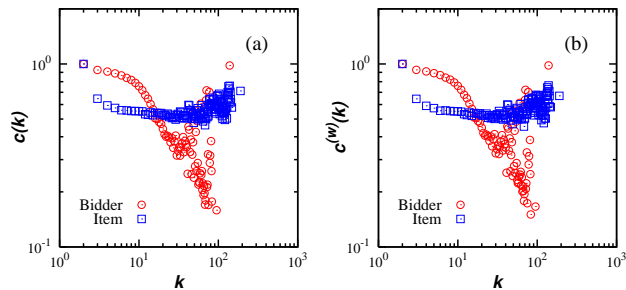


FIG. 7: Average clustering coefficient functions  $c(k)$  ( $\circ$ ) and  $c^{(w)}(k)$  ( $\square$ ) as a function of degree  $k$  for the bidder network (a) and the item network (b). The result implies that the bidder network is hierarchically organized, whereas the item network is almost random.

independent of  $k$ , which is shown in Fig. 7(b); this implies that the network is almost randomly organized. Such behaviors are observed irrespective of whether the networks are binary or weighted.

### III. CLUSTER IDENTIFICATION

By using network analysis, individual elements can be classified into clusters. Here, we apply the hierarchical agglomeration (HA) algorithm, which was introduced by Clauset *et al.* [19], to the item network containing 264,073 items. In particular, the algorithm is useful for a system containing a large number of elements. Clusters identified using this analysis are compared with traditional subcategories established based on off-line transactions. The obtained difference can be used for reorganizing a dendrogram with regard to item subcategories; this difference reflects the pattern of online bidding activities.

To realize this, we first store the topology of the item network by using the adjacent matrix  $\{a_{ij}\}$ . By maintaining this information, we delete all the edges, thereby leaving  $N$  isolated vertices. At each step, we select one edge from the stored adjacent matrix, which maximizes a change in the modularity, defined as

$$Q = \sum_{\alpha} e_{\alpha\alpha} - a_{\alpha}^2, \quad (5)$$

where  $e_{\alpha\alpha}$  is the fraction of the edges that connect the vertices within cluster  $\alpha$  on both the ends of each edge, and  $a_{\alpha}$  is the fraction of edges attached on one end or both the ends to vertices within cluster  $\alpha$ . The selected edge is eliminated from the stored matrix. We continue this edge-adding process until the modularity becomes maximum. We find that the modularity reaches the value  $Q_{\max} \approx 0.79$  for the item network and  $Q_{\max} \approx 0.83$  for the bidder network; this implies that both the networks are extremely well categorized. We recognize 1,904 and 870 distinct clusters in the bidder and item networks, respectively. The cluster sizes, the number of vertices of

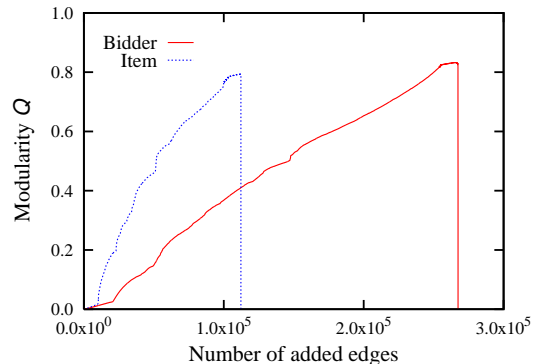


FIG. 8: The evolution of modularity  $Q$  by using the edge-adding process. The  $x$  axis represents the number of edges added. The maximum value obtained is estimated to be  $Q_{\max} = 0.83$  for the bidder network (solid line) and  $Q_{\max} = 0.79$  for the item network (dotted line).

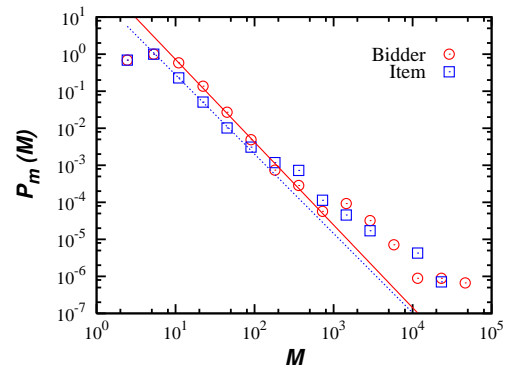


FIG. 9: The cluster-size distributions for the bidder and item networks, identified using the HA algorithm. The distributions follow the power law,  $P_m(M) \sim M^{-\tau}$  with  $\tau_B \approx 2.2$  and  $\tau_I \approx 2.1$ . The exponents are estimated from the region with the data in small  $M$ . Solid and dashed lines are guide-lines. The presented data are log-binned. Raw data in the region with large  $M$  are sparse.

each module, are not uniform. The cluster-size distributions for both networks, even though large deviations exist for a large cluster size  $M$ , exhibit fat-tail behaviors such that  $P_m(M) \sim M^{-\tau}$  with  $\tau_B \approx 2.2$  and  $\tau_I \approx 2.1$  roughly. The exponents are estimated from the data in the region with small  $M$ .

## IV. DENDROGRAM BASED ON ONLINE TRANSACTIONS

### A. Closeness

In this section, we focus on the item network. We have identified 870 distinct clusters by using the clustering algorithm. Among them, 49 clusters contain more than 100 items within each cluster. On the other hand, according to the traditional classification scheme, items in the eBay

auction are categorized into 18 categories which contains 192 subcategories. Obviously the clusters that we found are not equivalent to these categories or subcategories. Thus, our goal is to construct a new dendrogram, a hierarchical tree, among 192 subcategories based on the closeness between the obtained clusters and the existing subcategories.

To illustrate closeness, we select a cluster  $\alpha$  and classify the items within the cluster into 192 subcategories. The fraction of items in each subcategory  $\mu$  is the closeness  $C_{\alpha\mu}$ . For example, Fig. 10 shows the closenesses for the first five largest clusters. Each strip represents a cluster obtained from the HA algorithm. For each strip, the  $x$ -axis represents 192 subcategories, and the  $y$ -axis does the closeness. The bar indicates the closeness. For cluster 1, subcategory (a) exhibits the largest closeness. For cluster 2, subcategory (c) has the largest closeness, and so on. The abbreviations for the 18 main categories are as follows: *Antique* stands for antiques and art; *Biz*, business and office; *Clothes*, clothing and accessories; *Collect*, collectibles; *Comp*, computers; *Elec*, consumer electronics; *Dolls*, dolls and bears; *Home*, home and garden's; *Jewelry*, jewelry, gemstones and watches; *Glass*, pottery and glass; and *Estt*, real estate.

## B. Correlation matrix

To quantify the correlation, we adopt the method used for the clustering analysis for expression data from DNA microarrays. In this approach, we regard the closeness as the expression level, subcategories as genes, and clusters as different DNA microarray experiments [17].

The correlation matrix element  $\rho_{\alpha\beta}$  is defined as

$$\rho_{\alpha\beta} = \frac{\langle C_{\alpha\mu} C_{\beta\mu} \rangle - \langle C_{\alpha\mu} \rangle \langle C_{\beta\mu} \rangle}{\sqrt{(\langle C_{\alpha\mu}^2 \rangle - \langle C_{\alpha\mu} \rangle^2)(\langle C_{\beta\mu}^2 \rangle - \langle C_{\beta\mu} \rangle^2)}}, \quad (6)$$

where  $C_{\alpha\mu}$  represents the closeness of subcategory  $\mu$  ( $\mu = 1, \dots, n = 192$ ) to cluster  $\alpha$  ( $\alpha = 1, \dots, 870$ ) and  $\langle \dots \rangle$  denotes the average over different clusters indexed by  $\mu$ .

Based on the correlation matrix, a dendrogram that assembles all  $n = 194$  subcategories into a single tree can be constructed. For this purpose, we use the hierarchical clustering algorithm introduced by Eisen *et al.* [17]. We start the tree construction process by calculating the correlation coefficients  $\{\rho_{\alpha\beta}\}$  with size  $192 \times 870$ . Next, the matrix is scanned to identify a pair of subcategories with the highest value of the correlation coefficient, and the two subcategories are combined. Thus, a pseudo-subcategory is created, and its closeness profile is calculated only by averaging closenesses of the combined subcategories. This is referred to as the average-linkage clustering method. Then,  $n - 2$  isolated subcategories and a pseudo-subcategory remain. The correlation matrix is updated with these  $n - 1$  units and the highest correlation coefficient is found. The process is repeated  $n - 1$  times until only a single element

remains. After these steps, a dendrogram is constructed in which the height represents the magnitude of the correlation coefficient.

## C. Rearrangement of subcategories in the dendrogram

The resulting dendrogram is shown in the upper part of Fig. 11, which is considerably different from the traditional classification scheme shown in the lower part of this figure. We discuss the details of the correlations of the subcategories in the dendrogram. For discussion, we divide the entire tree structure into six branches, denoted by (A)–(F).

To be specific, branch (A) covers a broad range of different collectibles. The relationship between the subcategories may be attributed to collecting manias. Branch (B) mainly covers three types of subcategories: *clothing* and *accessories*, *business*, *office* and *industries*, and *sports* categories. Branch (C) consists of three parts: the first part has *antiquary property* and the items used for *decorating homes* and the second part covers very broad kinds of items. The third is interesting and covers a set of *electronic products* such as computers, cameras, audio players, etc. It also includes *video games* as well as *food* and *beverages*. At a glance, one may wonder how these two items are correlated; however, by considering the fact that some video games maniacs requires foods and beverages while playing, one can find the reason. Thus, the dendrogram indeed reflects the bidding patterns of individual bidders. Branch (D) covers items related to *artistic collections* and *hobbies*. Branch (E) covers *books*, *dolls* for children, etc. Finally, branch (F) mainly covers collectibles in a wide range from *jewelry* to *stamps*.

## V. CONCLUSIONS AND DISCUSSION

Based on the empirical data collected from the eBay web site, we have constructed a bipartite network comprising bidders and items. The bipartite network is converted into two single species of networks, the bidder and item networks. We measured various topological properties of each network. Both networks are scale free in the degree distribution. It is noteworthy that both the networks are assortatively mixed with regard to the degree correlation. This fact implies that the active bidders tend to simultaneously bid for common items; therefore, they are connected. Accordingly, attractive items are connected via such active bidders. Next, by applying the hierarchical agglomeration algorithm, we identified clusters in the bidder and item networks. The clusters are well separated from each other. Then, we calculate the correlation matrix between subcategories by using the information on the fraction of items in each subcategory in a given cluster. By using this correlation

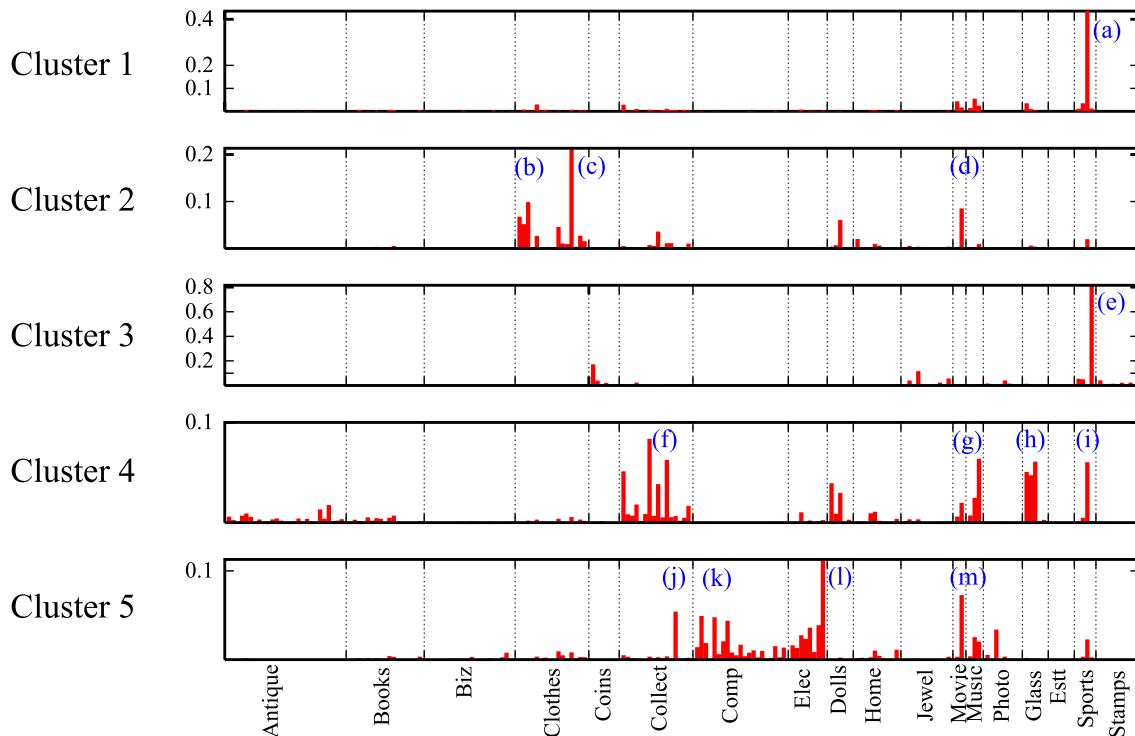


FIG. 10: The closeness between the clusters and subcategories. The  $x$ -axis represents the 192 subcategories and the  $y$ -axis represents the closeness. For the largest cluster (cluster 1), subcategory (a), Sports and Goods, exhibits the largest closeness. This result indicates that the main fraction of items in cluster 1 originates from subcategory (a), even though small fractions of items exist from other subcategories. For cluster 2, the subcategories of Clothing & Accessories (b), Women Clothing (c), and Movies (d) are the major fractions. The fact that these three subcategories belong to the same cluster implies that they are strongly correlated in an online transaction. For cluster 3, the subcategory of Sports Trading Cards (e) is dominant. For cluster 4, (f),(g),(h), and (i) subcategories exhibit a strongly correlation. For cluster 5, subcategories (j),(k),(l), and (m) are correlated, which represent the Pop Culture of Collectibles, Computers, Consumer Electronics, and Movies, respectively.

matrix, we construct the dendrogram, which is different from the traditional classification scheme. Based on a detailed investigation about the items closely located in the dendrogram, we find that the dendrogram indeed is bidder-oriented in an online auction. Therefore, the dendrogram could be useful for marketing renovation,

resulting in an increase in profits.

This work was supported by KRF Grant No. R14-2002-059-010000-0 of the ABRL program funded by the Korean government (MOEHRD).

- 
- [1] E. van Heck and P. Vervest, *Commun. ACM* **41**, 99 (1998).
- [2] R. D’Hulst and G.J. Rodgers, *Physica A* **294**, 447 (2001).
- [3] A.E. Roth and A. Ockenfels, *American Economic Review* **92**, 1093 (2002).
- [4] A. Kambil, Eric van Heck, and E. van Heck, *Making Markets: How firms can design and profit from online auctions and exchanges* (Harvard Business School Press, 2002).
- [5] I. Yang, H. Jeong, B. Kahng, and A.-L. Barabási, *Phys. Rev. E* **68**, 016102 (2003).
- [6] I. Yang and B. Kahng, arXiv:physics/0511073.
- [7] J. Reichardt and S. Bornholdt, arXiv:physics/0503138.
- [8] D. J. Power, *A Bi-Weekly Publication of DSSResources.COM*. <http://dssresources.com/newsletters/66.php>.
- [9] R. Albert and A.-L. Barabási, *Rev. Mod. Phys.* **74**, 47 (2002).
- [10] S. N. Dorogovtsev and J. F. F. Mendes, *Evolution of networks* (Oxford University Press, Oxford, 2003).
- [11] M. E. J. Newman, *SIAM Rev.* **45**, 167 (2003).
- [12] Girvan, M. and M. E. J. Newman, *Proc. Natl. Acad. Sci. USA* **99**, 7821 (2002).
- [13] M. E. J. Newman, *Phys. Rev. E* **69**, 066133 (2004).
- [14] R. Guimera, L. Danon, A. Diaz-Guilera, F. Giralt, and A. Arenas, *Phys. Rev. E* **68**, 065103(R) (2003).
- [15] A. Arenas and L. Danon, A. Diaz-Agulea, P. M. Gleiser, and R. Guimera, *Eur. Phys. J. B* **38**, 373 (2004).
- [16] M. Boguna, R. Pastor-Satorras, A. Diaz-Guilera, and A. Arenas, *Phys. Rev. E* **70**, 056122 (2004).

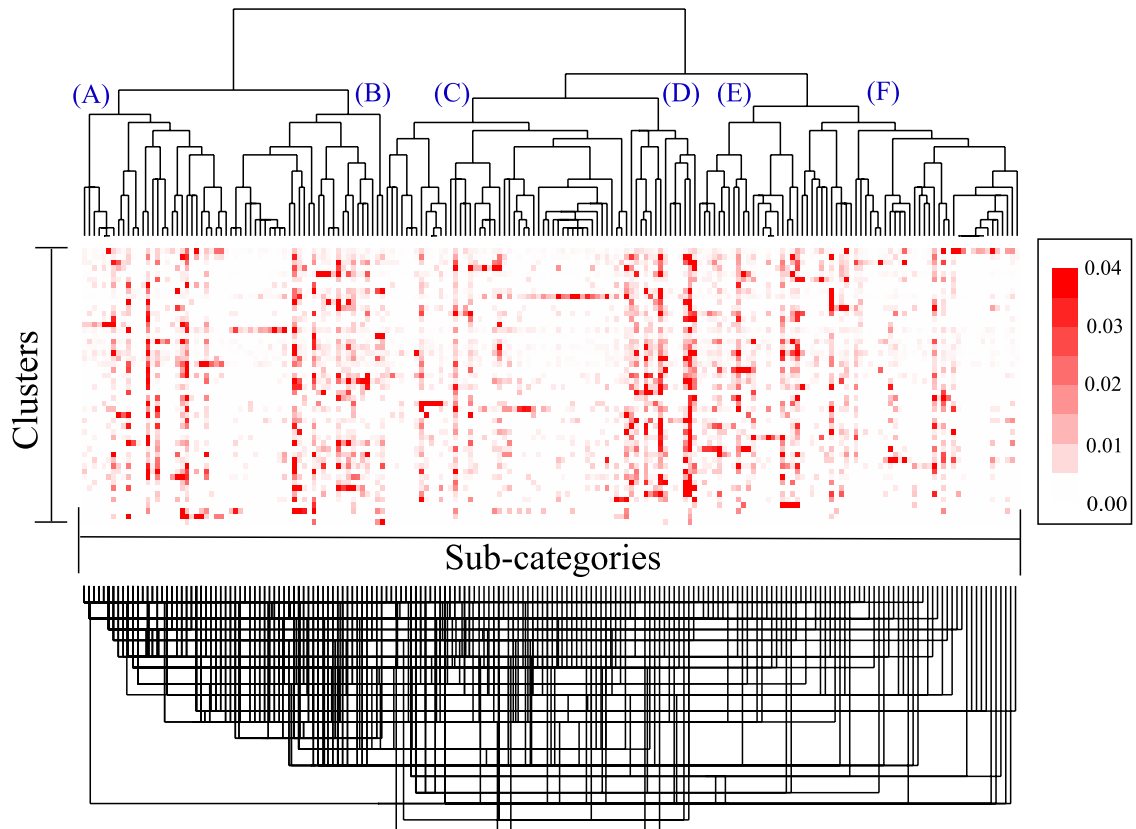


FIG. 11: Upper part: the dendrogram constructed by using the hierarchical clustering algorithm for the item network of an eBay online auction. Subcategories in branches (A)–(F) are explained in the text. Middle part: the closenesses of each subcategory for different clusters are shown with various concentrations. Lower part: the traditional classification scheme of subcategories in the version where original data were collected. The classification scheme is a bilayer structure comprising 18 categories and 192 subcategories. For visual clarity, however, the bilayer structure is shown in a multilayer manner. For comparison, the subcategories are in the same order as that used in the upper part. We can easily observe that the traditional classification scheme is entangled from the bidder-oriented perspective.

- [17] M. B. Eisen, P. T. Spellman, P. O. Brown, and D. Bostein, Proc. Natl. Acad. Sci. USA **95**, 14863 (1998).
- [18] A. Barrat, M. Barthelemy, R. Pastor, A. Vespignani, Proc. Natl. Acad. Sci. **101**, 3747 (2004).
- [19] A. Clauset, M.E.J. Newman, C. Moore, Phys. Rev. E **70**, 066111 (2004).